Opto-acoustic study of tinuvin-P and rhodamine 6G in solid polymeric matrices

S. Nonell[1,*]**, C. Martí**[1]**, I. García-Moreno**[2]**, Á. Costela**[2]**, R. Sastre**[3]

[1] CETS Institut Químic de Sarrià, Universitat Ramon Llull, Via Augusta 390, 08017 Barcelona, Spain
(Fax: +34-93/205-6266, E-mail: nonel@iqs.url.es)
[2] Instituto de Química Física Rocasolano, CSIC, Serrano 119, 28006 Madrid, Spain
(Fax: +34-91/564-2431, E-mail: iqrfm84@iqfr.csic.es and acostela@iqfr.csic.es)
[3] Instituto de Ciencia y Tecnología de los Polímeros, CSIC, Juan de la Cierva 3, 28006 Madrid, Spain
(Fax: +34-91/564-4853, E-mail: ictrs45@ictp.csic.es)

Abstract. Laser-induced opto-acoustic calorimetry has been used to examine the thermo-elastic properties of two polymer matrices doped with tinuvin-P and the radiation-less decay processes of rhodamine 6G (Rh6G) in them. The matrices assayed were methyl methacrylate (MMA) homopolymers P(MMA), and methyl methacrylate and 2-hydroxyethyl methacrylate (HEMA) copolymers P(MMA : HEMA). A slight difference in the thermo-elastic properties of the polymers, namely their adiabatic expansion coefficients, has been detected and found to correlate with the long-term stability of the laser material. This suggests a key role of the heat-dissipation processes in the photostability of these polymeric materials. On the other hand, the fluorescence quantum yield of Rh6G is shown to vary with the polymer-matrix composition in a way consistent with its lasing efficiency. The Rh6G absorption and fluorescence quantum yield also change dramatically upon increasing its concentration, which suggests the co-existence of different Rh6G forms with different photophysical properties.

PACS: 81.70.C; 42.70.H

The use of polymeric solid matrices as an alternative to conventional liquid-solution dye lasers has been extensively studied [1]. The large volumes required, flammability, solvent evaporation, flow fluctuation and toxicity are some of the disadvantages of liquid-solution dye lasers that would be ameliorated by the use of polymers as solid matrices.

Solid polymer–glass solutions of rhodamine 6G, Rh6G, have been synthesized and their lasing properties studied [1]. The photophysical properties (including the efficiency in laser operation) have been widely studied by means of fluorescence spectroscopy [2]. One of the main problems encountered upon the use of these solid matrices is the thermal- and/or photodegradation of the dye, tentatively explained in terms of the poor heat dissipation in the matrix [3–5]. Attempts to ameliorate this situation include the systematic variation of the polymer-matrix compo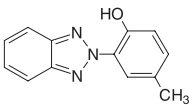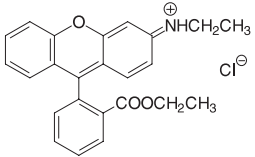sition and the covalent binding of the dye to the polymeric chain, both actions aimed at increasing the heat-dissipation rate [6–8].

Laser-induced opto-acoustic spectroscopy (LIOAS) is a calorimetric technique that monitors photo-induced volume changes resulting from fast radiation-less processes and chemical reactions (within ∼1 µs after the laser excitation pulse). For a given amount of heat released, the magnitude of the volume change observed is determined by the thermo-elastic properties of the medium, and can thus be used to obtain them. Additionally, from the ratio of heat released/energy absorbed, the fluorescence quantum yield of dyes can be determined. In this work we examine the opto-acoustic behavior of several solid polymer solutions of Rh6G. We validate the use of this technique for polymer matrices doped with tinuvin-P (tin-P) as a photocalorimetric standard. Tin-P is a widely used photostabilizer additive for polymeric materials [9–15] that de-activates in the picosecond time domain or even faster [14]. The detailed de-activation mechanism remains unclear, though formation of an intramolecular hydrogen bond plays a central role [13–15].

The present paper reports the preparation of and the application of the LIOAS technique to different polymer matrices containing Rh6G or tin-P at different concentrations (listed in Table 1) for the determination of their thermo-elastic properties and of the fluorescence quantum yield of Rh6G in them. The particular laser materials chosen for our study were solid solutions of Rh6G in copolymers of methyl methacrylate (MMA) and 2-hydroxyethyl methacrylate (HEMA) with MMA : HEMA compositions of 1 : 1 and 7 : 3 vol/vol, P(MMA : HEMA). These materials were chosen because in a previous study [7] significant variations in the lasing characteristics with the copolymer composition were appreciated. Whereas in the Rh6G/P(MMA : HEMA 1 : 1) samples the lasing efficiency was 21.5% with a lifetime (measured as the number of pulses that produce an 80% drop in the laser output) of 8500 pulses for pumping at 337 nm at a 2-Hz repetition rate, in the Rh6G/P(MMA : HEMA 7 : 3) material the efficiency and lifetime dropped to 11.5% and 5000 pulses, respectively [7]. It has been suggested [1] that the thermal properties of the matrix should play an important role in the lasing characteristics of solid-state dye lasers.

---

*Corresponding author.

Table 1. List of samples

	Matrix	Concentration/μM
	P(MMA)	0
		1
		2
		5
		10
		20
TIN-P		
	P(MMA : HEMA 1 : 1)	0
		1
		2
		4
		10
		20
		100
	P(MMA : HEMA 1 : 1)	12
		50
Rh6G	P(MMA : HEMA 7 : 3)	12

Thus, we have applied the LIOAS technique to investigate the thermo-elastic properties of the sample and the fluorescence of Rh6G, and determine if there is a direct relationship between them and their lasing efficiency and photostability.

1 Materials and methods

1.1 Materials

2-hydroxy-benzophenone (2HBP, Aldrich), dichloromethane (SDS, spectroscopic grade), tin-P [2-(2′-hydroxy-5′-methylphenyl)benzotriazole, supplied by Ciba Specialty Chemicals as a gift] and Rh6G chloride [o-(6-ethylamino-3-ethylimino-2,7-dimethyl-3H-xanthene-9-yl) benzoic acid ethyl ester, Lambda Physik] were used as received. Monomers HEMA (Alcolac) and MMA were vacuum-distilled under nitrogen and stored in a cool dark place. MMA (99%) was previously washed with 10% aqueous sodium hydroxide to remove the inhibitor, followed by washing with water and drying over sodium sulfate.

In the preparation of the polymeric dye samples, the precise amount of the corresponding dye was first added to freshly purified HEMA or MMA and the resulting mixture was placed in an ultrasonic bath until complete dissolution of the dye. In the copolymers, pure MMA was then added as well as a quantity of 1.5 g/L of 2,2′-azobis(isobutyronitrile), AIBN, used as a free-radical initiator, and the mixture was again sonicated. AIBN is the thermal polymerization initiator of choice, since it leaves UV-transparent end groups on the obtained polymer or copolymer. A number of monomer mixtures with different volume/volume proportions of HEMA and MMA were prepared. The resulting solution was filtered into appropriate cylindrical polypropylene molds using a 0.45-μm-pore-size filter followed by a 0.2-μm-pore-size

filter (Whatman Lab. PTFE disposable filters). After careful de-aeration by bubbling dry argon for 10 min, the molds were sealed. An inert atmosphere avoids the well-known oxygen inhibition of radical polymerization. Polymerization was performed in the dark at 400 °C over a period of 2 days and then at 450 °C for about 1 day. The temperature was then raised to 600 °C and increased slowly up to 800 °C over a period of several days, in order to decompose residual AIBN. Finally, the temperature was reduced and only then the sample was unmolded. This procedure was essential in order to reduce the buildup of stresses in the polymer samples due to thermal shock. The solid samples were cut to the appropriate shape for opto-acoustic experiments, i.e. a side-truncated cylindrical block with front and back windows prepared by conventional grinding and polishing until of optical-grade finish. The flat side window allowed for optimal acoustic contact with the piezo-electric transducer.

1.2 Methods

Absorption spectra were measured with a Varian Cary 4 E spectrophotometer, periodically calibrated with a holmium oxide filter from Hellma.

The formation of nanosecond or longer-lived transients and of singlet oxygen, $O_2(^1\Delta_g)$, was examined with time-resolved laser techniques, namely nanosecond laser flash photolysis and time-resolved near-IR phosphorescence detection, respectively. These systems have been described in detail elsewhere [16]. The set-up for LIOAS is similar to that described previously [17]. Briefly, a N_2 laser (emitting at 337 nm) was used to irradiate the solid samples mounted on a home-made holder that allowed for sample replacement with minor disturbance of the system geometry. It is well known that the shape and magnitude of the opto-acoustic signal is extremely sensitive to the acoustic contact between sample and transducer. Our holder allowed for very good reproducibility of the acoustic contact (signals were reproducible within 4%). The beam of the N_2 laser was concentrated with the aid of a 50-cm cylindrical lens and a 100-cm lens, and shaped to a 1-mm wide × 3-mm high rectangle with the aid of a slit placed immediately in front of the sample. A small fraction of the beam was diverted to a pyro-electric-head-based energy meter (Laser Precision Corporation RJ-7610 with RjP-735 probe) in order to determine the amount of laser energy per pulse. It was kept routinely under 12 μJ with the aid of suitable neutral density filters. The pressure wave generated in the sample was detected at 90° with a 1-MHz piezo-electric transducer. Its output was fed to a 150-MHz Lecroy 9410 digital oscilloscope and transferred to a PC for storage and analysis. Typically 100 shots were averaged for each sample. The amplitude difference between the first maximum and minimum of the pressure wave, ΔH, was measured as a function of the laser energy for each sample in order to locate the linear-response region. For a purely thermal signal the amplitude of the opto-acoustic wave is related to the fraction, α, of absorbed energy released as heat within the time window of the experiment, which in our case was ~ 1 μs (1) [18, 19]:

$$\Delta H = K \cdot \Delta V = K \frac{\beta}{c_p \cdot \varrho} \cdot E_1 \cdot (1 - 10^{-A}) \cdot \alpha, \qquad (1)$$

where: K is a proportionality constant that includes geometric and electronic parameters of the detection system; ΔV is the photo-induced volume change; β, c_p and ϱ are the thermoelastic parameters of the medium, i.e. the isobaric thermal expansion coefficient, the specific heat capacity and the density, respectively; the function $\beta/c_p\varrho$ is often called the adiabatic expansion coefficient; E_l is the laser energy; and A is the absorbance of the sample at the excitation wavelength.

The calorimeter is calibrated with a reference in the same medium which is assumed to release all the energy absorbed as prompt heat ($\alpha = 1$) and with an absorbance matched to that of the sample. Thus, the α value for the sample is obtained as:

$$\alpha_{\text{sample}} = \frac{\Delta H_{\text{sample}}}{\Delta H_{\text{ref}}} \,. \tag{2}$$

In practice, one measures ΔH is a function of the laser energy and of the sample absorption factor $1 - 10^{-A}$ and uses the slope of the linear plots obtained as an energy- and absorption-normalized amplitude. When the sample contains more than one chromophore, the opto-acoustic signal is the sum of the contributions of each chromophore; hence the measured α value is the absorbance average of the individual α values for each chromophore:

$$\alpha = \sum \frac{A_i \alpha_i}{A_{\text{total}}} \,. \tag{3}$$

The α value provides a valuable insight into the photophysical properties of the chromophore. Thus, the difference between the energy absorbed and the energy released as prompt heat provides the sum of the energy lost in radiative processes, e.g. fluorescence, plus the energy dissipated in longer time scales, i.e. that 'stored' in a long-lived transient such as a triplet state:

$$E_\lambda(1 - \alpha) = E_F \cdot \Phi_F + E_{\text{st}} \cdot \Phi_{\text{st}} \,, \tag{4}$$

where E_λ is the energy content of the laser photons, $E_F \Phi_F$ the average energy released as fluorescence and $E_{\text{st}} \Phi_{\text{st}}$ the energy stored in a long-lived transient.

2 Results and discussion

2.1 Absorbance of tin-P at 337 nm in the polymer matrices

Figure 1 shows the absorption spectra for tin-P in MMA : HEMA 1 : 1 copolymers measured versus air in the reference-beam pathway. Similar plots were obtained for the homopolymer matrices, P(MMA). The band centered at approximately 340 nm, corresponding to the planar form of tin-P [13], is mounted on a falling background signal. The Beer–Lambert plot at 337 nm (cf. inset) is strictly linear, thus confirming that the samples are true homogeneous solutions where tin-P is in a monomeric form. From the slopes, the absorption coefficients are obtained as $(14.4 \pm 0.5) \times 10^3 \, \text{M}^{-1}\text{cm}^{-1}$ for the P(MMA) homopolymer and $(15.0 \pm 0.5) \times 10^3 \, \text{M}^{-1}\text{cm}^{-1}$ for the 1 : 1 copolymer, which compare favorably with the values reported by Keck et al. for tin-P covalently bound to MMA in liquid toluene solutions, $16.7 \times 10^3 \, \text{M}^{-1}\text{cm}^{-1}$ at 345 nm [14]. The non-zero intercept in the Beer–Lambert plot indicates that the beam is attenuated by other mechanisms as well,
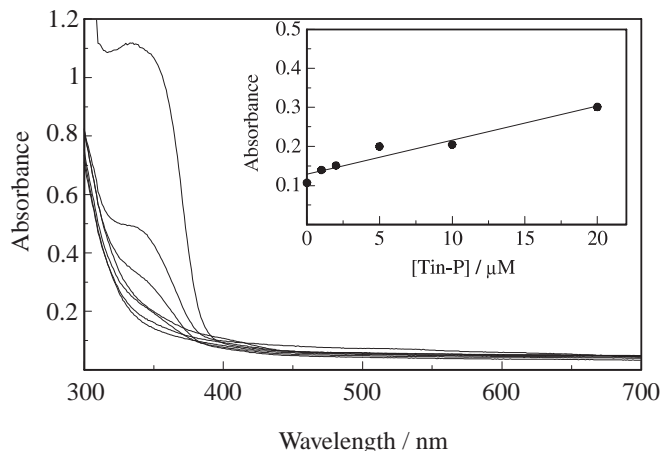
Fig. 1. Absorption spectra for tin-P in MMA : HEMA(1 : 1) copolymer, measured versus air. The concentrations are listed in Table 1. *Inset*: Beer–Lambert plot at 337 nm

which include surface reflection and polymer absorption and scattering. The intercept, D, thus provides the polymer attenuance. We find that it is matrix-dependent and equal to $D = 0.336$ for the homopolymer and $D = 0.147$ for the 1 : 1 copolymer at 337 nm. Hence, the absorbance read is actually the polymer attenuance plus the tin-P absorbance. The latter can then be obtained by simple subtraction of the intercept. We will need it when interpreting the opto-acoustic results.

### 2.2 Opto-acoustic behavior of tin-P in the polymer matrices

Using laser flash photolysis, we did not observe any transients in the ns–ms range. No singlet oxygen was observable either with the more sensitive time-resolved near-infrared phosphorescence detection, which would be indicative of formation of triplet states of tin-P, as in systems where the hydrogen bond is disrupted [12]. We also failed to observe any fluorescence and the samples were photostable over long irradiation periods. We then conclude that tin-P de-activates in the sub-nanosecond time scale exclusively through non-radiative channels and that it has negligible photochemistry in our polymers.

Figure 2 shows the opto-acoustic amplitude for tin-P in the 1 : 1 copolymer as a function of the energy of the laser pulses. As expected, linear plots are obtained, thus ruling out the presence of unwanted effects such as ground-state depletion or multiphotonic absorption.

In Fig. 3a the energy-normalized opto-acoustic amplitudes (ΔH_E) – the slopes of the energy plots – are shown as a function of the sample attenuance D (the read absorbance) for both matrices. According to (1), a linear relationship should be obtained. This is indeed the case, though a negative intercept is also apparent. This most likely shows that the 'true' absorbance of the sample, to which the LIOAS technique is sensitive, is lower than its attenuance, which is not surprising as the polymer reflects, scatters and perhaps also absorbs light. Using the tin-P absorbance (see above) instead of the total attenuance yields also a straight line but now with positive intercept. This indicates that the polymer is indeed an additional chromophore and absorbs light at 337 nm. Its absorbance can be determined using the zero-intercept criterion, i.e. a constant value is added to the tin-P
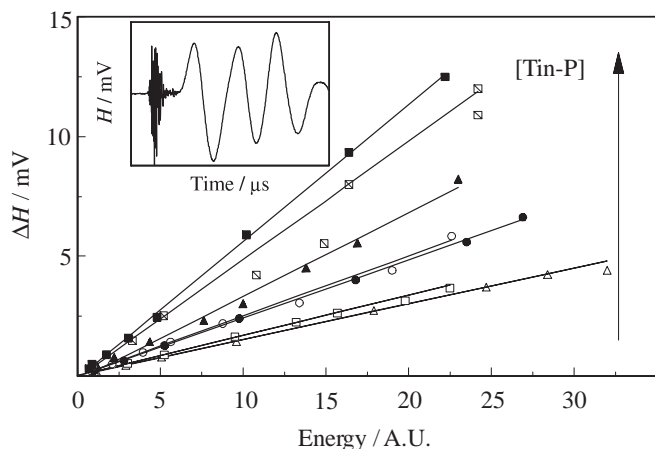
Fig. 2. Laser-energy dependence of the opto-acoustic maximum amplitude for tin-P in MMA : HEMA copolymers at 0 (△), 1 (□), 2 (●), 4 (○), 10 (▲), 20 (⊠) and 100 μM (■). $\lambda_{exc} = 337$ nm. Error bars $\sim 5\%$. *Inset*: Typical opto-acoustic signal
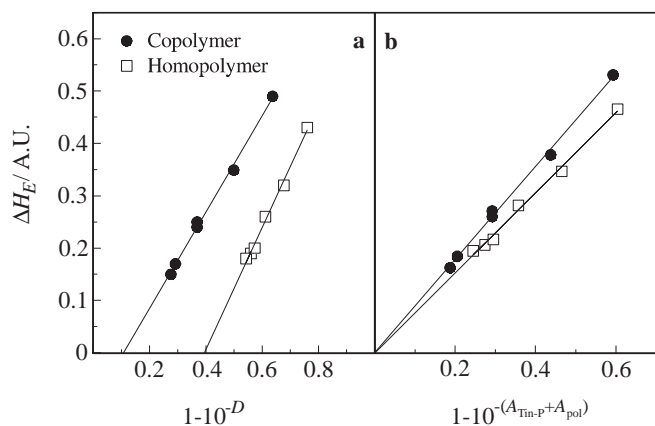
Fig. 3. a Energy-normalized opto-acoustic amplitude as a function of the sample attenuance (absorption + reflection + scattering) for tin-P in P(MMA) and in P(MMA : HEMA 1 : 1). **b** Energy-normalized opto-acoustic amplitude as a function of the sample absorbance (tin-P + polymer; see text) in P(MMA) and in P(MMA : HEMA 1 : 1) matrices. Error bars $\sim 5\%$

absorbance until the plots go through zero (Fig. 3b). We find that the absorbance is $A_{pol} = 0.118$ for the homopolymer and $A_{pol} = 0.090$ for the 1 : 1 copolymer, which can lead to a significant filter effect for diluted Rh6G polymer glasses when pumped by a nitrogen laser at 337 nm. As we also failed to observe any transient behavior for the neat polymer, we can assume that it is photochemically stable, thus acting as a calorimetric reference just as tin-P. Taking the attenuance at 700 nm as a measure for the polymer reflection, we can calculate the attenuance due to scattering at 337 nm. The values for absorption, reflection and scattering contributions to the polymer attenuance at 337 nm are collected in Table 2
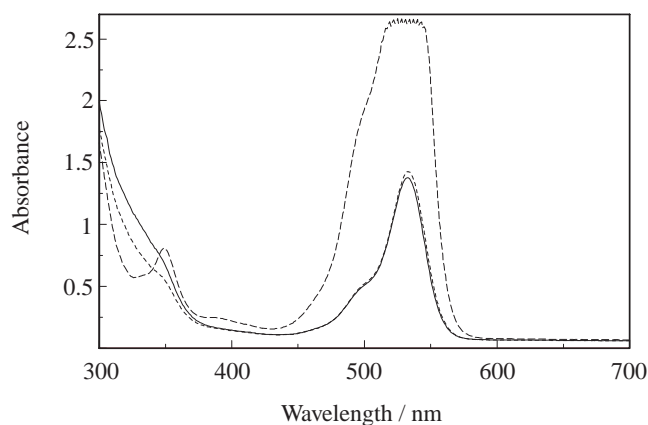
and will be used for the interpretation of the Rh6G results (see below).

2.3 Thermo-elastic properties of the polymers

Figure 3b shows different slopes for the two polymers. According to (1), the slopes are proportional to the thermo-elastic coefficients of the polymers ($\beta/c_p\varrho$, or volume increment per absorbed energy). We therefore conclude that the 1 : 1 copolymer is $\sim 16\%$ more expandable than the homopolymer P(MMA). It could be expected that further increases of HEMA proportion in the sample would lead to a continuous increase of the thermal expansion coefficient of the matrix with the corresponding improvement in the photostability of the dye dissolved in the final material. In fact, previous results revealed that by increasing the HEMA content from 30% to 50% the lifetime of the Rh6G dissolved in the laser material increased from 5000 to 8500 laser pulses [7]. While this can not be taken as a definite proof of the role of the thermo-elastic properties of the matrix in the photostability of the solid polymer, the agreement is sufficiently striking as to warrant further exploration of the matrix composition.

2.4 Opto-acoustic behavior of Rh6G in polymer matrices

Figure 4 shows the absorption spectrum for Rh6G in copolymers MMA : HEMA 1 : 1 and 7 : 3 at concentrations of 12 and 50 μM (see Table 1). Especially in the 300−350-nm region, the absorption spectrum is matrix- and concentration-dependent. We then anticipate that the photophysics and perhaps also the lasing properties of Rh6G will be influenced by their local environment, which is in agreement with the

Fig. 4. Absorption spectra of Rh6G 12 μM (———) and 50 μM (– – –) in P(MMA : HEMA 1 : 1) and 12 μM (– – –) in P(MMA : HEMA 7 : 3)

Table 2. Attenuance at 337 nm and thermo-elastic properties of the polymer glasses

| Matrix | Attenuance at 337 nm | | | Relative thermo-elastic properties |
	Absorbance	Reflection and scattering	Total	$(\beta/c_p\varrho)$/A.U.
P(MMA)	0.118	0.290	0.408	1
P(MMA : HEMA 1 : 1)	0.090	0.093	0.183	1.16

Table 3. Summary of photophysical results obtained for Rh6G. $\lambda_{exc} = 337$ nm

Polymer matrix	[Rh6G]	A_{total}	A_{pol}	A_{Rh6G}	ΔH_E	α	α_{Rh6G0}	Φ_F
P(MMA : HEMA 1 : 1)	12 μM	0.63	0.09	0.54	0.48	0.76	0.72	0.46
P(MMA : HEMA 1 : 1)	50 μM	0.41	0.09	0.32	0.27	0.54	0.41	0.97
P(MMA : HEMA 7 : 3)	12 μM	0.48	0.10	0.38	0.42	0.81	0.76	0.39

previous experimental observations [2]. The absorbance of Rh6G has been calculated by subtracting the polymer attenuance (absorption, reflection and scattering, cf. Table 2) from the measured attenuance at 337 nm. The results are collected in Table 3. As no data is available for the 7 : 3 copolymer, we assume that the polymer absorbance is proportional to the HEMA content, and thus calculate it by linear interpolation between the values for the homopolymer and the 1 : 1 copolymer, i.e. $A_{pol} \sim 0.10$ for the 7 : 3 copolymer.

The opto-acoustic amplitude for all Rh6G samples was, as for tin-P, linear with the laser energy. The slopes of these energy plots are collected in Table 3. The comparison of these slopes with those of tin-P at the same total absorbance (dye + polymer, obtained by interpolation in Fig. 3b) allows the determination of the α value for the Rh6G polymers by means of (2). These values are also collected in Table 3. The thermo-elastic properties for the 7 : 3 copolymer have been estimated by interpolation between those of the homopolymer and the 1 : 1 copolymer assuming linearity with the HEMA content, i.e. $(\beta/c_p\varrho)_{P(MMA:HEMA\ 7:3)} \sim 1.10(\beta/c_p\varrho)_{P(MMA)}$.

The α values for the three samples are significantly lower than 1, implying that Rh6G loses part of the absorbed energy by other channels, in agreement with the fluorescence results by López Arbeloa et al. [2]. As for tin-P, we failed to observe any transient or singlet oxygen; hence we assume that under these experimental conditions and within the temporal window selected in this work fluorescence is the main additional de-activation channel, which is of course consistent with their use as laser dyes. As two different chromophores are present in the sample, namely Rh6G and the polymer, we can use (3) to calculate the α value for Rh6G as:

$$\alpha_{Rh6G} = \frac{\alpha \cdot A_{total} - \alpha_{pol} \cdot A_{pol}}{A_{Rh6G}} . \qquad (5)$$

Assuming $\alpha_{pol} = 1$ (see above), the α_{Rh6G} values are readily calculated and collected in Table 3. It can be appreciated that, for a given dye concentration, more absorbed energy is released as heat in the P(MMA : HEMA 7 : 3) matrix than in the P(MMA : HEMA 1 : 1) one. Consequently, in a laser experiment the energy available to appear as laser emission would be lower in the first material and as a result the Rh6G/P(MMA : HEMA 7 : 3) sample should be less efficient. This is indeed the case: when samples of Rh6G incorporated into copolymers of MMA and HEMA were pumped at 337 nm in a laser configuration the lasing efficiency of the Rh6G/P(MMA : HEMA 1 : 1) samples was found to be nearly double the efficiency of the Rh6G/P(MMA : HEMA 7 : 3) samples [7].

Similar results were obtained by Costela et al. using a non-linear optical technique [20]. These authors performed studies on thermally induced phase conjugation by degenerate four-wave mixing in copolymers of MMA and HEMA doped with Rh6G, and were able to estimate the fraction α of the absorbed light energy converted into heat. For a dye concentration 10^{-3} M and irradiation wavelength of 432 nm

they found α values of 0.36 and 0.27 for the Rh6G/P(MMA : HEMA 7 : 3) and Rh6G/P(MMA : HEMA 1 : 1) samples, respectively, indicating that more energy appears as heat in the first material, in agreement with the results obtained here using the LIOAS technique.

Equation 4 can now be used to obtain the fluorescence quantum yields for Rh6G in these polymers. Using the fluorescence maximum for Rh6G as 554 nm for both matrices [2], (4) can be rewritten as:

$$\Phi_F = (1 - \alpha_{Rh6G}) \cdot \frac{554}{337} , \qquad (6)$$

which leads to the Φ_F values collected in Table 3.

At the concentration 12 μM, the parameter Φ_F decreases slightly as the HEMA content in the matrix increases. The same trend was observed in previous work where the fluorescence quantum yield of Rh6G dissolved in these polymeric matrices was evaluated by the phase-conjugated technique [20]. More to the point, the dependence of Φ_F on the matrix composition follows the same behavior as the lasing efficiencies that are reported for the Rh6G in the two polymers pumped at 337 nm, namely 21% for the 1 : 1 copolymer and 11.5% for the 7 : 3 polymer [7].

We find that for the 1 : 1 copolymer, increasing the concentration from 12 to 50 μM induces a ca. two-fold increase in Φ_F. This suggests the co-existence of at least two different forms of Rh6G with different photophysical properties, the relative proportion of these forms in the matrix being concentration-dependent. Concentration and matrix-composition effects in Φ_F were already observed by López Arbeloa et al. [2], though they observed the opposite trend, i.e. a reduction of Φ_F. However, they excited at 495 nm; hence it is likely that the proportion of the co-existing Rh6G forms being photo-excited was different than in our case.

As pointed out in the introductory section of this paper, the laser properties of Rh6G in the MMA : HEMA 1 : 1 and 7 : 3 copolymers are quite different, with significant increases in both efficiency and photostability in the 1 : 1 copolymer. The LIOAS measurements summarized in Tables 2 and 3 provide thermo-elastic properties of the polymer matrices and fluorescence quantum yields that correlate with the laser properties. Thus, the differences in laser behavior between both materials can be explained in terms of differences in these basic physicochemical properties, though other degradation processes cannot be ruled out [21–23].

3 Conclusions

Laser-induced opto-acoustic calorimetry has been used to examine the thermo-elastic properties of two polymer matrices and the radiation-less decay processes of Rh6G in them. A slight difference in the thermo-elastic properties of the polymers has been detected and it correlates with the long-term stability of the laser material. On the other hand, the

fluorescence quantum yield of Rh6G is found to vary with the polymer-matrix composition in a way consistent with its lasing efficiency. The Rh6G absorption and fluorescence quantum yield also change dramatically upon increasing its concentration, which suggests the co-existence of different Rh6G forms with different photophysical properties.

References

1. A. Costela, I. García-Moreno, J.M. Figuera, F. Amat-Guerri, R. Sastre: Laser Chem. **18**, 63 (1998)
2. F. López Arbeloa, T. López Arbeloa, I. López Arbeloa, A. Costela, I. García-Moreno, J.M. Figuera, F. Amat-Guerri, R. Sastre: Appl. Phys. B **64**, 651 (1997)
3. I.P. Kaminow, L.W. Stulz, E.A. Chandross, C.A. Pryde: Appl. Opt. **11**, 1563 (1972)
4. I.P. Kaminow, H.P. Weber, E.A. Chandross: Appl. Phys. Lett **18**, 497 (1971)
5. R.L. Fork, Z. Kaplan: Appl. Phys. Lett **20**, 472 (1972)
6. F. Amat-Guerri, A. Costela, J.M. Figuera, R. Sastre: Chem. Phys. Lett. **209**, 352 (1993)
7. A. Costela, F. Florido, I. García-Moreno, R. Duchowicz, F. Amat-Guerri, J.M. Figuera, R. Sastre: Appl. Phys. B **60**, 383 (1995)
8. A. Costela, I. García-Moreno, J.M. Figuera, F. Amat-Guerri, R. Sastre: Appl. Phys. Lett **68**, 593 (1996)
9. J. Catalán, J.L.G. de Paz, M.R. Torres, J.D. Tornero: J. Chem. Soc. Faraday Trans. **93**, 1691 (1997)
10. J. Catalán, F. Fabero, M.S. Guijarro, R.M. Claramunt, M.D. Santa María, M.C. Foces-Foces, F. Hernández Cano, J. Elguero, R. Sastre: J. Am. Chem. Soc. **112**, 747 (1990)
11. J. Catalán, J. Palomar, J.L.G. de Paz: J. Phys. Chem. A **101**, 7914 (1997)
12. P.F. McGarry, S. Jockusch, Y. Fujiwara, N.A. Kaprinidis, N.J. Turro: J. Phys. Chem. A **101**, 764 (1997)
13. K.P. Ghiggino, A.D. Scully, S.W. Bigger: *Effects of Radiation on High-Technology Polymers* (381 ACS Symposium Series, Washington, DC 1989)
14. J. Keck, H.E.A. Kramer, H. Port, T. Hirsch, P. Fischer, G. Rytz: J. Phys. Chem. **100**, 14468 (1996)
15. C.M. Estevez, R.D. Bach, K.C. Hass, W.F. Schneider: J. Am. Chem. Soc. **119**, 5445 (1997)
16. B. del Rey, U. Keller, T. Torres, G. Rojo, F. Agulló-López, S. Nonell, C. Martí, S. Brasselet, I. Ledoux, J. Zyss: J. Am. Chem. Soc. **120**, 12808 (1998)
17. C. Martí, O. Jürgens, O. Cuenca, M. Casals, S. Nonell: J. Photochem. Photobiol. A: Chem. **97**, 11 (1996)
18. S.E. Braslavsky, G.E. Heibel: Chem. Rev. **92**, 1381 (1992)
19. S.E. Braslavsky, K. Heihoff: *CRC Handbook of Photochemistry*, Vol. 1 (CRC, Boca Raton 1989)
20. A. Costela, J.M. Figuera, F. Florido, I. García-Moreno, R. Sastre: Opt. Commun. **119**, 265 (1995)
21. A. Costela, I. García-Moreno, J.M. Figuera, F. Amat-Guerri, R. Mallavia, M.D. Santa-María: J. Appl. Phys. **80**, 3167 (1996)
22. K.M. Dyumaev, A. Manenkov, A.P. Maslyukov, G.A. Matyushin, V.S. Nechitailo, A.M. Prokhorov: J. Opt. Soc. Am. B **9**, 143 (1992)
23. S. Popov: Appl. Opt. **37**, 6449 (1998)